Rapport d'activité scientifique

Laboratoire DynFluid

Année 2021

Table des matières

Effectifs permanents/non permanents pour l'année 2021

— **Permanents :**

1. Nicolas ALFEREZ – Maître de Conférences CNAM,
2. Damien BIAU – Maître de Conférences ENSAM,
3. Ismaïl BEN HASSAN SAÏDI – Enseignant-Chercheur contractuel ENSAM (A partir du 01/09),
4. Virginie DARU – Maître de Conférences/HDR ENSAM,
5. Xavier GLOERFELT – Professeur des Universités ENSAM,
6. Francesco GRASSO – Professeur émérite,
7. Simon MARIE – Maître de Conférences/HDR CNAM,
8. Xavier MERLE – Maître de Conférences ENSAM,
9. Jean-Christophe LOISEAU – Maître de Conférences ENSAM,
10. Jean-Christophe ROBINET – Professeur des Universités ENSAM.
11. Luca SCIACOVELLI – Maître de Conférences ENSAM,

— **Ingénieurs de Recherche :**

1. Junior JUNQUEIRA – ENSAM,
2. Dan HLEVCA – CNAM,

— **ATER/postdoctorats :**

1. Camille GOUIN, Sept. 2021 - Sept. 2022, ATER/CNAM,
2. Gabriele NASTRO, Jan. 2021 - dec. 2022, CleanSky/PERSEUS,
3. Özgür YALCIN, Déc. 2021 - dec. 2022, CleanSky/PERSEUS,

— **Doctorants :**

1. Soufiane CHERROUD, Oct. 2020 - Sept. 2023, CD-ENSAM,
2. Maximilien DE ZORDO-BANLIAT, Dec. 2018 - Nov. 2021, CIFRE/SAFRANTECH,
3. Valentin FER, Oct. 2019 - Sept. 2022, ONERA,
4. Ricardo FRANTZ, Nov. 2018 - Oct. 2021, CD-ENSAM,
5. Antoine JOUIN, Oct. 2019 - Sept. 2022, Politecnico di Bari,
6. Enza PARENTE, Oct. 2018 - Sept. 2021, Politecnico di Bari,
7. Donatella PASSIATORE, Oct. 2018 - Sept. 2021, Politecnico di Bari,
8. Aurélien BIENNER, Fév. 2021 - Fev. 2024, ANR REGAL-ORC,
9. Mathieu SALMON, Oct. 2021 - Sept. 2024, ONERA,
10. Alessando FRANCHINI, Nov. 2021 - Oct. 2024, DGAC
11. Camille MATAR, Nov. 2021 - Oct. 2024, CD-Sorbonne U.

— **Stagiaires :**

1. Donato VARIALE (01 Mars - 31 Août),
2. Angelo MARTUCCI (01 Mars - 31 Août),

Objectifs scientifiques du laboratoire DynFluid

Le laboratoire DynFluid (équipe d'accueil EA 92) est un laboratoire en cotutelle Arts et Métiers ParisTech / Conservatoire National des Arts et Métiers. Il mène des travaux de recherche en Mécanique des fluides, Aérodynamique et Acoustique, avec des applications dans les secteurs aéronautique, automobile et celui des procédés industriels. Il développe des méthodes numériques originales pour simuler des écoulements et des phénomènes aéroacoustiques, ou analyser leurs instabilités et il met en œuvre ces méthodes dans le cadre de programmes de recherche nationaux ou internationaux. Le laboratoire collabore également avec de nombreux partenaires industriels et académiques.

Les thèmes du laboratoire sont les suivants :

Thème 1 : Multi-Espèces & Thermodynamiques complexes (MET)

Animateur : Simon Marié (CNAM)

Thème 2 : Compressibles, Turbulence & Acoustique (CTA)

Animateur : Xavier Gloerfelt (ENSAM)

Thème 3 : Machine Learning & Quantification d'incertitude (MLQ)

Animateur : Xavier Merle (ENSAM)

Thème 4 : Instabilités, Transition & Contrôle (ITC)

Animateur : Damien Biau (ENSAM)

Inter-groupe : GTNum

Animateur : Carlos Junqueira Junior (ENSAM)

Séminaires Externes & Internes

Animateur : Damien Biau (ENSAM)

Première partie

Multi-Espèces & Thermodynamiques complexes (MET)

Décroissance de turbulence homogène et isotrope en Novec^{TM}649

Aurélien BIENNER (doctorant) & Xavier GLOERFELT
Collaborations : P. Cinnella (SU), S. aus der Wiesche (Univ. Muenster)

L'objectif est de réaliser un calcul de décroissance de turbulence homogène et isotrope (THI) pour le gaz dense Novec^{TM}649, dans les conditions expérimentales de la soufflerie CLOWT (ANR franco-allemande Regal-ORC). Ce calcul servira de référence pour le dimensionnement d'une expérience de décroissance de turbulence de grille qui sera ensuite réalisée par l'équipe de l'université de Muenster dans leur soufflerie CLOWT. La turbulence réalisée permettra de contrôler les conditions amont pour une transition de type 'freestream' sur une plaque ou une aube représentative des turbines ORC.

Une première campagne de simulations a permis de mettre en place la méthode numérique qui sera utilisée par la suite. La méthode utilisée a été validée en utilisant les résultats expérimentaux de Comte-Bellot & Corrsin en air (gaz parfait). La figure 4 montre qu'un bon accord est obtenu pour une grille fine de 512^3. On pourra ensuite réduire le maillage en utilisant la simulation des grandes échelles.

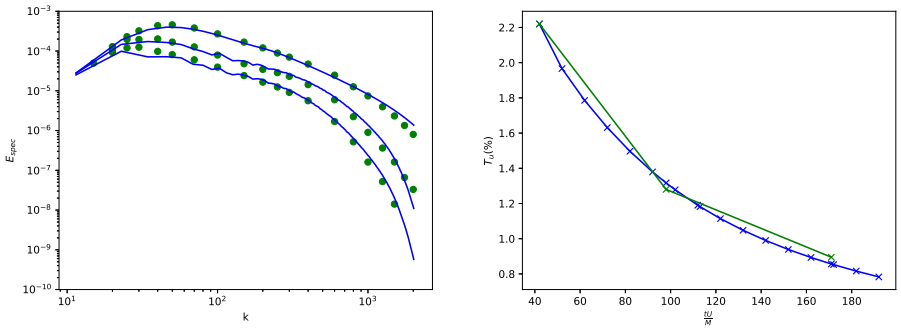

FIGURE 1 – Décroissance de THI en air (configuration de Comte-Bellot & Corrsin) sur une grille de 512^3. À gauche, spectres d'énergies unidimensionnelles en aval de la grille aux stations $tU/M = 42$, $tU/M = 98$ et $tU/M = 171$. À droite, évolution du taux de turbulence T_u en fonction de la distance à la grille. Bleu : simulation. Vert : expérience pour une taille de maille $m = 5.08\,\text{cm}$.

Pour le calcul en gaz dense, on utilise le Novec^{TM}649 pour des conditions typiques de la soufflerie CLOWT (100°C et 4 bars), qui fonctionne en haut subsonique. Il existe cependant très peu d'expérience de décroissance de turbulence de grille en régime compressible et la simulation numérique est utilisée pour préfigurer les conditions d'expériences. Ainsi la taille de maille m minimale possible serait autour de 1 mm. Comme le gaz est dense (masse volumique d'environ 50 kg/m^3 dans les conditions précédentes pourtant assez éloignées du point critique), le challenge pour la simulation est que des grands nombres de Reynolds sont rapidement atteints. Ainsi pour Mach=0.5, le Reynolds de maille Re_m est 130 000 pour m=1 mm et le double pour m=2 mm (qui réduit le blocage sonique pour ces vitesses haut subsoniques), à comparer à $Re_m = 34\,000$ dans l'expérience de Comte-Bellot & Corrsin. Une DNS est alors hors de portée (environ 8000^3). Des calculs de décroissance de THI avec 1024^3 points ont été réalisés pour le Novec^{TM}649. D'autres simulations seront nécessaires, notamment pour étudier l'influence du modèle de sous-maille et pour effectuer ce qui sera la première comparaison avec les données expérimentales pour une THI de gaz dense.

Transition de couches limites en Novec^{TM}649

Aurélien BIENNER (doctorant) & Xavier GLOERFELT
Collaborations : P. Cinnella (SU), S. aus der Wiesche (Univ. Muenster)

Dans le cadre du projet ANR-DFG REGAL-ORC, nous aurons accès aux premières données fines pour la transition d'une couche limite de gaz dense (Novec^{TM}649, Mach=0.9) dans la boucle de retour CLOWT de notre partenaire allemand, l'université de Münster. Il s'agit d'une boucle pressurisée (4 bar, 100°C) et, compte-tenu de la grande densité du fluide réfrigérant utilisé (ρ_{Novec649}=48.5 kg/m^3), des nombres de Reynolds élevés sont atteints sur une plaque de 6 cm de long. Le défi est de mettre en place une instrumentation miniaturisée et des simulations numériques permettront une première validation croisée pour ce gaz dense.

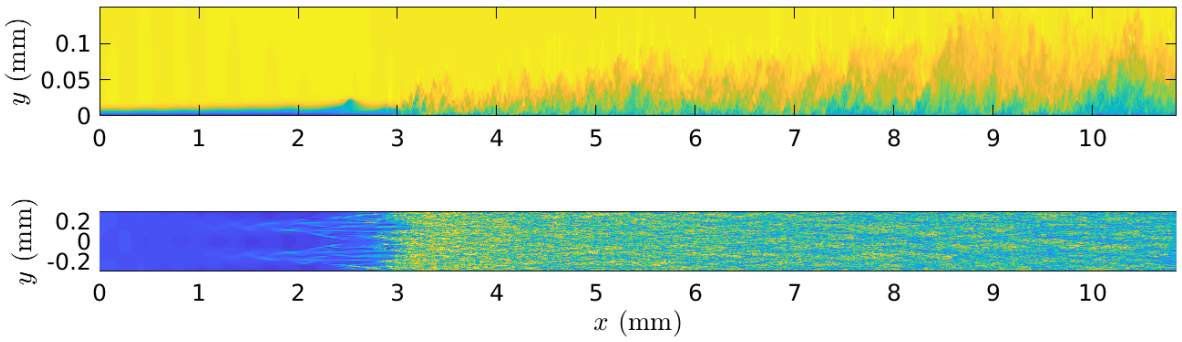

FIGURE 2 – Simulation numérique directe de la transition oblique d'une couche limite de Novec^{TM}649 à M=0.9 (3.6 milliards de points, 5 millions hCPU sur 18000 procs ; instantané de la vitesse longitudinale).

Il est prévu de réaliser une expérience en soufflerie pour la transition free-stream en Novec^{TM}649 (100°C et 4 bars) et de réaliser des simulations numériques pour affiner les analyses. Afin de mettre en place cette campagne d'essais expérimentaux et numériques, nous choisissons de commencer par une transition modale (avec un premier mode oblique) à Mach 0.9 par simulation numérique directe (DNS). Il s'agira d'une solution de référence pour guider le montage expérimental et les futures simulations. Un calcul DNS a permis notamment de tester des maillages plus légers (Wall-resolved LES), indispensables pour pouvoir faire une étude paramétrique de la transition free-stream (méthode de génération de turbulence amont, taux de turbulence Tu, échelle intégrale des structures de la turbulence amont, ...). La DNS a également permis de valider la réduction du coût de calcul avec un avancement temporel implicite IRS.

Communication :

[1] A. Bienner, X. Gloerfelt & P. Cinnella, Numerical study of boundary-layer transition in a high-subsonic organic vapor flow, *56th 3AF International Conference AERO2022*, Toulouse, 2022.

[2] A. Bienner, X. Gloerfelt, P. Cinnella, L. Hake, S. aus der Wiesche & S. Strehle, Study of bypass transition in dense-gas boundary layers, *12th International Symposium on Turbulence and Shear Flow Phenomena*, Osaka (online), 2022.

Dense gas flow past a cylinder

Camille MATAR (doctorant) & Xavier GLOERFELT
Collaborations : P. Cinnella (SU), S. aus der Wiesche (Univ. Muenster)

In the frame of the ANR-DFG project Regal-ORC, an assessment of measurement technique suitability for compressible organic vapour flows is ongoing, such as circular Pitot probe or hot-wire anemometry. The working fluid used in the wind tunnel is Novec^{TM}649, a fluorinated ketone. In the master thesis of Camille Matar, the dense gas flow around the cylinder has been studied numerically with the unsteady Reynolds-Averaged Navier-Stokes equations method (URANS) to validate pressure measurements on its surface at high Reynolds numbers in the range $10^5 \leq Re_D \leq 6.1 \times 10^6$. The free-stream Mach number was comprised between 0.1 and 0.65. The URANS is found to be in reasonably good agreement with wall pressure measurements and to perform better than RANS at most of the considered conditions, but discrepancies persist and the results are very sensitive to the development of the turbulent wake. Recently, the team of Prof. aus der Wiesche has produced time-resolved Schlieren pictures of compressible cylinder at Mach numbers of 0.6/0.7 and Reynolds number of $3 \times 10^5/6 \times 10^5$. Our goal is then to replicate one of such experiments using LES. At these high-subsonic conditions, weak shock waves develop on either sides of the cylinder, which are very sensitive to non-ideal gas effects. The LES will be compared with Schlieren data and pressure measurements obtained at Univ. Muenster as well as with our previous RANS and URANS results.

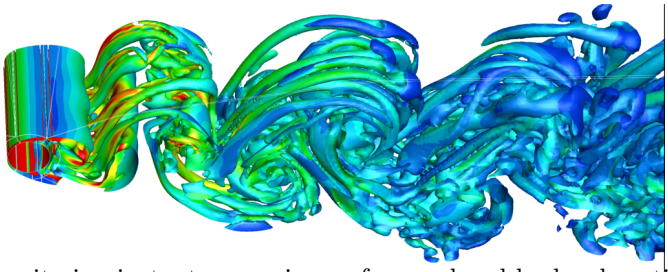

FIGURE 3 – Q-criterion instantaneous iso-surfaces colored by local vorticity magnitude.

In the thesis of Camille Matar, started in oct. 2021, low-Reynolds LES have been carried out for cylinder geometries representative of a hot-wire. The Reynolds numbers were in the range $700 \leq Re_D \leq 1500$ which enabled us to simulate the three-dimensional flow with LES. The figure shows the development of turbulent structures in the wake at Re_D=717 and Mach number M=0.67. At such low Reynolds, flow remains very coherent in the near wake, but breaks down to turbulence around 2D downstream the cylinder.

Communications :

[1] P. Cinnella, C. Matar, X. Gloerfelt, F. Reinker & S. aus der Wiesche, High subsonic organic vapor flow past a circular cylinder, *6th International Seminar on ORC Power Systems*, Munich, Germany, 2021.

[2] L. Hake, L. Sundermeier, L. Cakievski, J. Bäumer, S. aus der Wiesche, C. Matar, P. Cinnella & X. Gloerfelt, Hot-wire anemometry in high subsonic organic vapor flows, *ASME Turbo Expo 2022 Turbomachinery Technical Conference and Exposition*, Rotterdam, Netherlands, 2022.

Thermochemical non-equilibrium effects in turbulent hypersonic boundary layers

Donatella PASSIATORE (doctorante) & Luca SCIACOVELLI
Collaborations : P. Cinnella (SU), Giuseppe PASCAZIO (Politecnico di Bari)

A hypersonic, spatially evolving turbulent boundary layer at Mach 12.48 with a cooled wall is analysed by means of direct numerical simulations. At the selected conditions, massive kinetic-to-internal energy conversion triggers thermal and chemical non-equilibrium phenomena. Air is assumed to behave as a five-species reacting mixture, and a two-temperature model is adopted to account for vibrational non-equilibrium. Wall cooling partly counteracts the effects of friction heating, and the temperature rise in the boundary layer excites vibrational energy modes while inducing mild chemical dissociation of oxygen. Vibrational non-equilibrium is mostly driven by molecular nitrogen, characterized by slower relaxation rates than the other molecules in the mixture. The results reveal that thermal non-equilibrium is sustained by turbulent mixing : sweep and ejection events efficiently redistribute the gas, contributing to the generation of a vibrationally under-excited state close to the wall, and an over-excited state in the outer region of the boundary layer. The tight coupling between turbulence and thermal effects is quantified by defining an interaction indicator. A modelling strategy for the vibrational energy turbulent flux is proposed, based on the definition of a vibrational turbulent Prandtl number. The validity of the strong Reynolds analogy under thermal non-equilibrium is also evaluated. Strong compressibility effects promote the translational–vibrational energy exchange, but no preferential correlation was detected between expansions/compressions and vibrational over-/under-excitation, as opposed to what has been observed for unconfined turbulent configurations.

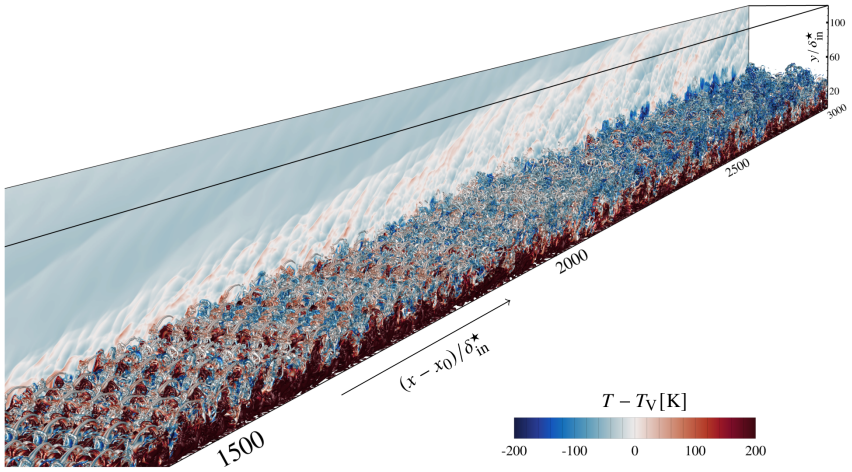

FIGURE 4 – Instantaneous isocontours of $T - T_V$ in a xy-plane and second invariant of the velocity gradient tensor, Q, coloured by $T - T_V$.

Communication :

[1] D. Passiatore, L. Sciacovelli, P. Cinnella & G. Pascazio. Thermochemical non-equilibrium effects in turbulent hypersonic boundary layers,*Journal of Fluid Mechanics*, vol 941, A21, 2022.

Deuxième partie

Compressible, Turbulence & Acoustique (CTA)

Large-Eddy Simulations of Supersonic Jet Flows

Carlos JUNQUEIRA-JUNIOR
Collaborations : D. F. ABREU (doctorant / Instituto Tecnológico de Aeronáutica) ;
E. T. V. DAURICIO (doctorant / Instituto Tecnológico de Aeronáutica) and
J. L. F. AZEVEDO (Instituto de Aeronáutica e Espaço)

The present study is interested in the large-eddy simulation (LES) of supersonic jet flows. The work addresses specifically the simulation of a perfectly expanded free jet flow with a jet exit Mach number of 1.4 and temperature equal to the ambient temperature. At the moment, the work focuses on LES calculations with a discontinuous Galerkin method, using different mesh refinements and polynomial degrees, ranging from 50 to 410 million degrees of freedom (DOFs). Preliminary results are included in the present document and they indicate that the increasing *hp* refinement provides better agreement with experimental data. Computations with the largest number of DOFs here addressed are still running and they will be included the future versions of the report. The expectation is that the complete analysis can provide further insight into the requirements for the adequate simulations of such flows.

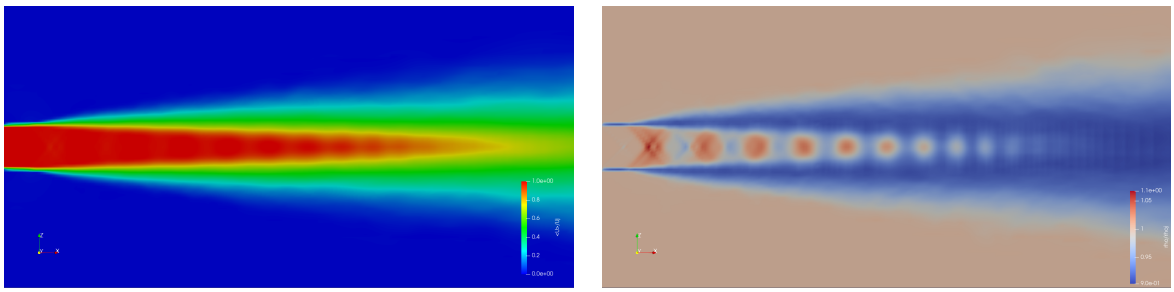

(a) Contours of longitudinal velocity component (b) Contours of mean density

FIGURE 5 – Contours of mean longitudinal velocity component on cutplane, (a) and contours of mean density (b), both in $z/D = 0$ for the refined simulation.

Publications et communications :

[1] Abreu, D.F., Junqueira-Junior, C., Dauricio, E.T.V., and Azevedo, J.L.F., "A Comparison of Low and High-Order Methods for the Simulation of Supersonic Jet Flows," Proceedings of the 26th ABCM International Congress of Mechanical Engineering – COBEM 2021, Paper COB-2021-0388, ABCM, Rio de Janeiro, Virtual Congress, 22–26 November 2021 (10 pages ; doi ://10.26678/ABCM.COBEM2021.COB2021-0388).

[2] Abreu, D.F., Junqueira-Junior, C., Dauricio, E.T.V., and Azevedo, J.L.F., "Study on the Resolution of Large-Eddy Simulations for Supersonic Jet Flows," Accepted to the 2022 AIAA Aviation Forum.

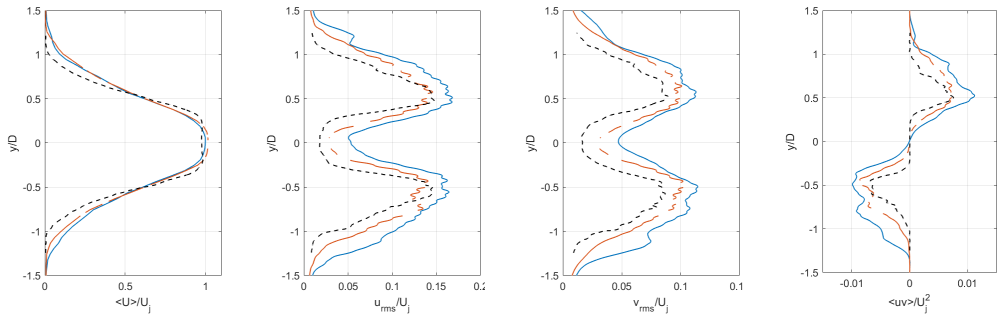

(a) (b) (c) (d)

FIGURE 6 – Profiles of mean streamwise velocity component (a), RMS of streamwise velocity fluctuation (b), RMS of radial velocity fluctuation (c), and mean Reynolds shear-stress tensor component (d) at $x/D = 5$.

Analysis of Shock-Boundary Layer Interactions in Adiabatic and Isothermal Supersonic Turbine Cascades

Carlos JUNQUEIRA-JUNIOR
Collaborations : H. F. S. LUI (doctorant / UNICAMP) ; T. R. RICCIARDI (postdoctorant / UNICAMP) and W. R. WOLF (UNICAMP)

A high-order overset compressible large-eddy simululation (LES) methodology is employed to solve the flow in a supersonic turbine cascade with different thermal boundary conditions. In this extended abstract, results are shown for adiabatic wall conditions. Spanwise and time averaged skin-friction and pressure coefficients are presented to investigate the mean flow behavior of the separation bubble. On the suction side, the separation bubble is 2 times larger than that on the pressure side. Then, power spectral density of the separation bubble length signal is provided to examine the low-frequency dynamics of the shock-boundary layer interaction (SBLI). Characteristic frequencies of the low-frequency unsteadiness are captured and results are consistent with previous studies on SBLI. Furthermore, the spanwise and time averaged $z-$vorticity contours at different time instants along with the velocity streamlines are presented to investigate the shear layer and separation bubble dynamics. Snapshots show the contraction and dilatation of the separation bubble as well the fluctuations of the shear layer. The authors will compare the adiabatic and isothermal wall configurations to investigate the effects of wall cooling on the SBLI in turbine cascades.

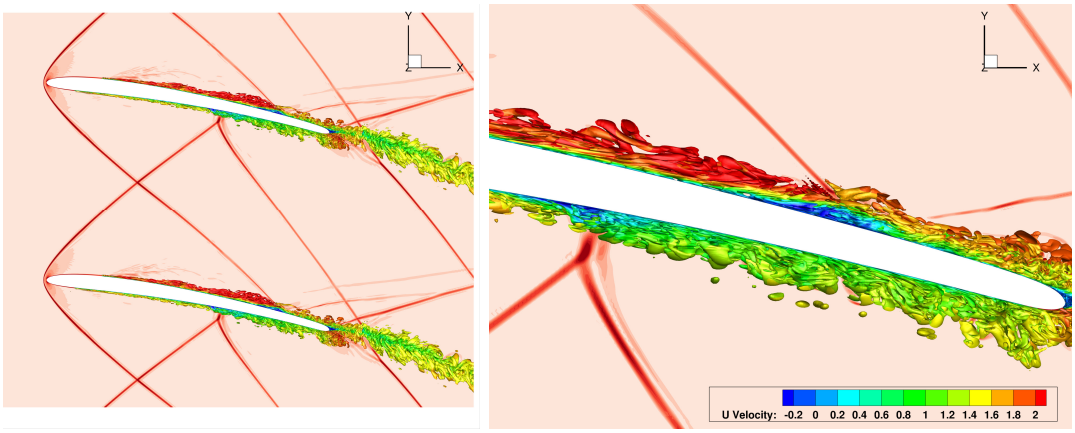

(a) Full view of linear cascade.

(b) Detail view of SBLIs.

FIGURE 7 – Iso-surfaces of Q-criterion colored by u-velocity component. The background plane displays the shock waves by visualizing the density gradient magnitude $|\nabla\rho|$.

Publications et communications :

[1] Lui, H. F. S., Ricciardi, T. R., Wolf, W. R., and Junqueira-Junior, C., "SAnalysis of Shock-Boundary Layer Interactions in Adiabatic and Isothermal Supersonic Turbine Cascades," Accepted to the 2022 AIAA Aviation Forum.

Code MUSICAA : avancement temporel implicite IRS

Aurélien BIENNER (doctorant) & Xavier GLOERFELT
Collaborations : P. Cinnella (SU)

En 2021, le code MUSICAA a été profondément modifié afin de gagner en généricité et d'intégrer de nombreuses fonctionnalités présentes dans une suite de solveurs. Cette réécriture vise à disposer d'une seule version du code capable de simuler des configurations multi-blocs massivement parallèles. MUSICAA est un code différences-finies d'ordre élevé avec transformation de coordonnées et l'aspect multi-bloc est géré par MPI. Une nouvelle fonctionnalité est la mise en place d'une méthode d'avancement temporel implicite. Les restrictions sur le pas de temps maximum autorisé pour les méthodes explicite d'intégration en temps peuvent s'avérer relativement sévères pour des simulations de type DNS et LES à haut nombre de Reynolds, en particulier à cause des maillages très raffinés près des parois pour capturer les structures turbulentes. Un moyen pour augmenter la stabilité est d'utiliser des schémas implicites d'intégration en temps, ce qui en contrepartie augmente le temps de calcul par itération, les erreurs de discrétisation et qui diminue la scalabilité en parallèle des calculs. Ainsi, l'IRS (Implicit Residual Smoothing), schéma d'intégration temporel à mi-chemin entre un schéma explicite et un schéma complètement implicite, apparaît comme un bon compromis. Une version à l'ordre 4 (IRS4) utilisant un lissage avec un bilaplacien a été proposée dans notre laboratoire (Cinnella & Content, JCP2016).

Case	Δt^+	$\frac{t_{CPU,expl.}}{t_{CPU,case}}$
Explicit	1.05×10^{-2}	1.0
IRS4	5.26×10^{-2}	4.06

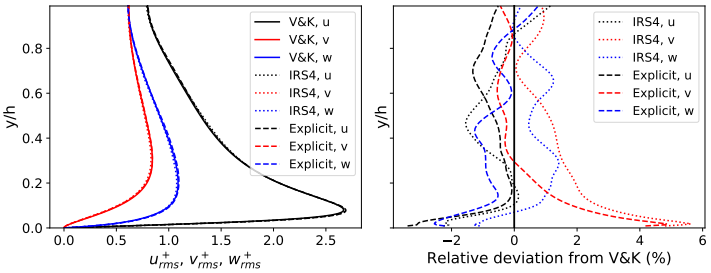

FIGURE 8 – Comparison of the rms velocities profiles with the Vreman & Kuerten (V&K) reference for the explicit and IRS4 time integrations with $\Delta t^+_{\text{IRS4}}=5 \times \Delta t^+_{\text{explicit}}$.

Une version différence-finie de cette méthode a donc été développée et implémentée dans le code MUSICAA, et notamment la possibilité de l'appliquer sur des maillages curvilignes. La figure montre que l'on peut multiplier le nombre de CFL par un facteur 5 pour le cas du canal plan turbulent sans occasionner trop d'erreur. Le lissage IRS induit un surcoût modéré (environ 15% par direction), essentiellement la résolution d'un système pentadiagonal par direction pour l'IRS4, si bien que des gains en temps de calcul de l'ordre de 4 sont attendus. La difficulté rencontrée est la parallélisation efficace de ces inversions pentadiagonales.

Communication :

[1] A. Bienner, X. Gloerfelt & P. Cinnella, Assessment of a high-order implicit residual smoothing time scheme for multiblock curvilinear meshes, *The 11th International Conference on Computational Fluid Dynamics*, Maui, 2022.

Couplage entre le streaming de Rayleigh et le transfert de chaleur à fort niveau acoustique dans un résonateur.

Virginie DARU
Collaborations : C. Weisman, D. Baltean-Carlès (SU), H. Bailliet (Institut P', Poitiers)

Le couplage entre les effets thermiques et l'écoulement moyen (classiquement streaming de Rayleigh) dans un guide d'ondes stationnaires est analysé théoriquement et numériquement. L'approche numérique est guidée par l'étude théorique. Cette dernière démontre que des tourbillons tournant en sens inverse du streaming de Rayleigh peuvent se former si le nombre de Reynolds de l'écoulement moyen dépasse une valeur dépendant de la fréquence des ondes et des propriétés thermophysiques du fluide, ainsi que de la paroi solide entourant le résonateur. Cette étude analytique démontre également l'importance de la présence d'une paroi conductrice d'épaisseur non nulle. Une configuration numérique est introduite afin d'étudier l'évolution de la structure de l'écoulement moyen et du champ de température moyenne à des niveaux acoustiques élevés. Cette configuration permet d'éviter dans la simulation l'apparition d'ondes de choc, qui ont un fort impact sur le champ de température moyenne alors qu'elles sont absentes dans les expériences. La conduction thermique est prise en compte dans la paroi du résonateur. Au fur et à mesure que le niveau acoustique augmente, on observe que le champ de température moyenne se stratifie transversalement. Les simulations montrent la pertinence du critère développé analytiquement pour caractériser l'apparition de nouvelles cellules de streaming contrarotatives à proximité des ventres de vitesse acoustique. Pour des niveaux acoustiques plus élevés, ces nouvelles cellules évoluent en des zones stagnantes de plus en plus étendues où la vitesse de l'écoulement moyen est très faible, et les contours de température sont stratifiés longitudinalement. Les résultats analytiques et numériques sont cohérents entre eux, ainsi qu'avec les observations expérimentales, montrant que le couplage intrinsèque entre les effets thermiques et le champ acoustique à des niveaux élevés est très bien décrit par le critère théorique et les simulations numériques.

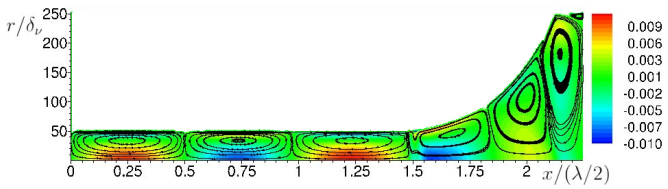

FIGURE 9 – Contours de la vitesse axiale de streaming (m s^{-1}) et lignes de courant de l'écoulement de streaming, sur le domaine de simulation entier, à faible niveau acoustique.

Publications :

[1] V. Daru, C. Weisman, D. Baltean-Carlès & H. Bailliet, « Acoustically induced thermal effects on Rayleigh streaming », J. Fluid Mech. vol. 911, A7, 2021.

[2] V. Daru, C. Weisman, D. Baltean-Carlès & H. Bailliet, « A numerical study of the coupling between Rayleigh streaming and heat transfer at high acoustic level », J. of the Acoustical Society of America 150(6), p. 4501-4510, 2021.

Troisième partie

Machine Learning & Quantification d'incertitude (MLQ)

Identifying stochastic differential equations with Langevin regression

Jean-Christophe LOISEAU
Collaborations : Steven L. BRUNTON (UW, Seattle, USA), Jared CALLAHAM (UW, Seattle, USA), Georgios Rigas (Imperial College, UK)

Systems characterized by nonlinear multiscale interactions can be effectively modeled by treating unresolved degrees of freedom as random fluctuations. Yet, even when the microscopic governing equations and qualitative macroscopic behavior are known, it is often difficult to derive a stochastic model consistent with observations. This is especially true for systems such as turbulence where the perturbations do not behave like Gaussian white noise, introducing non-Markovian behavior to the dynamics. We address these challenges with a framework for identifying interpretable stochastic nonlinear dynamics from experimental data, using both forward and adjoint Fokker-Planck equations to enforce statistical consistency. If the form of the Langevin equation is unknown, a simple sparsifying procedure can provide an appropriate functional form. This method can effectively learn stochastic models in two artificial examples : recovering a nonlinear Langevin equation forced by colored noise and approximating the second-order dynamics of a particle in a double-well potential with the corresponding first-order bifurcation normal form. Finally, it is applied to experimental measurements of a turbulent bluff body wake and show that the statistical behavior of the center of pressure can be described by the dynamics of the corresponding laminar flow driven by nonlinear state-dependent noise.

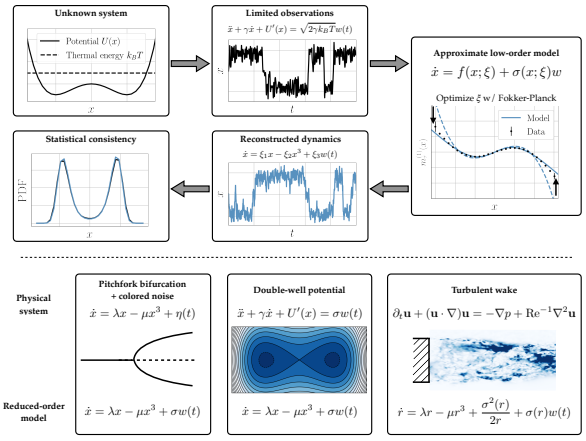

FIGURE 10 – Schematic of Langevin regression. Given a long time series of a macroscopic variable desribing a complex system, we seek to identify an approximate stochastic model. Langevin regression uses both the forward and adjoint Fokker-Planck operators to optimize free parameters of the model, ensuring consistency with observed statistics.

On the importance of nonlinear correlations for reduced-order modeling

Jean-Christophe LOISEAU
Collaborations : Steven L. BRUNTON (UW, Seattle, USA), Jared CALLAHAM (UW, Seattle, USA)

This work investigates nonlinear dimensionality reduction as a means of improving the accuracy and stability of reduced-order models of advection-dominated flows. Nonlinear correlations between temporal proper orthogonal decomposition (POD) coefficients can be exploited to identify latent low-dimensional structure, approximating the attractor with a minimal set of driving modes and a manifold equation for the remaining modes. By viewing these nonlinear correlations as an invariant manifold reduction, this least-order representation can be used to stabilize POD-Galerkin models or as a state space for data-driven model identification. In the latter case, we use sparse polynomial regression to learn a compact, interpretable dynamical system model from the time series of the active modal coefficients. We demonstrate this perspective on a quasiperiodic shear-driven cavity flow and show that the dynamics evolve on a torus generated by two independent Stuart-Landau oscillators. The specific approach to nonlinear correlations analysis used in this work is applicable to periodic and quasiperiodic flows, and cannot be applied to chaotic or turbulent flows. However, the results illustrate the limitations of linear modal representations of advection-dominated flows and motivate the use of nonlinear dimensionality reduction more broadly for exploiting underlying structure in reduced-order models.

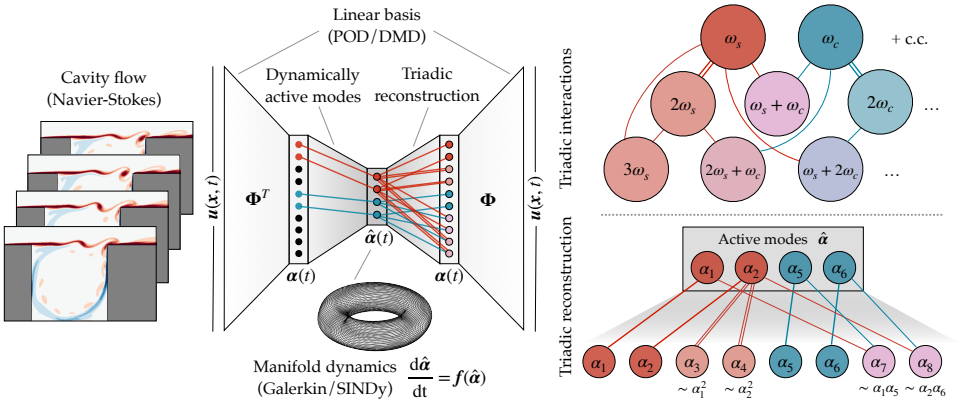

FIGURE 11 – Schematic of the model reduction approach exploiting nonlinear correlations. The flow fields are first projected onto a linear modal basis $\mathbf{\Phi}$, yielding modal coefficients $\boldsymbol{\alpha}(t)$. The quasiperiodic dynamics can be described by four degrees of freedom ; the rest of the modal coefficients can then be reconstructed with polynomial functions consistent with triadic interactions in the frequency domain. The dynamics of the active degrees of freedom can be modeled either by restricting the POD-Galerkin dynamics to the toroidal manifold or by identifying a simple, interpretable dynamical system with the SINDy algorithm.

CFD-driven Symbolic Identification of Algebraic Reynolds-Stress Models

Ismaïl BEN HASSAN SAÏDI, Francesco GRASSO
Collaborations : Paola CINNELLA (Sorbonne Université, Institut Jean Le Rond d'Alembert), Martin SCHMELZER (Delft University of Technology, The Netherlands)

A CFD-driven deterministic symbolic identification algorithm for learning explicit algebraic Reynolds-stress models (EARSM) from high-fidelity data is developed building on the frozen-training SpaRTA algorithm of. Corrections for the Reynolds stress tensor and the production of transported turbulent quantities of a baseline linear eddy viscosity model (LEVM) are expressed as functions of tensor polynomials selected from a library of candidate functions. The CFD-driven training consists in solving a blackbox optimization problem in which the fitness of candidate EARSM models is evaluated by running RANS simulations. The procedure enables training models against any target quantity of interest, computable as an output of the CFD model. Unlike the frozen-training approach, the proposed methodology is not restricted to data sets for which full fields of high-fidelity data, including second flow order statistics, are available. However, the solution of a high-dimensional expensive blackbox function optimization problem is required. Several steps are then undertaken to reduce the associated computational burden. First, a sensitivity analysis is used to identify the most influential terms and to reduce the dimensionality of the search space. Afterwards, the Constrained Optimization using Response Sur-face (CORS) algorithm, which approximates the black-box cost function using a response surface constructed from a limited number of CFD solves, is used to find the optimal model parameters. Model discovery and cross-validation is performed for three configurations of 2D turbulent separated flows in channels of variable section using different sets of training data to show the flexibility of the method. The discovered models are then applied to the prediction of an unseen 2D separated flow with higher Reynolds number and different geometry. The predictions of the discovered models for the new case are shown to be not only more accurate than the baseline LEVM, but also of a multi-purpose EARSM model derived from purely physical arguments. The proposed deterministic symbolic identification approach constitutes a promising candidate for building accurate and robust RANS models customized for a given class of flows at moderate computational cost.

Publications et communications :

[1] Ben Hassan Saïdi, I., Cinnella, P., and Grasso, F., "CFD-driven Sparse Identification of Algebraic", Aero2020+1, Poitiers, France, April 12-13-14 2021.

[2] Ben Hassan Saïdi, I., Cinnella, P., and Grasso, F., "Turbulence modeling using CFD-driven Symbolic Identification", Euromech colloquium, Paris, France, June 16-17-18 2021.

[3] Ben Hassan Saïdi, I., Schmelzer, M., Cinnella, P., and Grasso, F., "CFD-driven Symbolic Identification of Algebraic Reynolds-Stress Models", Journal of Computational Physics, Volume 457, 15 May 2022, 111037.

Machine Learning for turbulence modeling

Xavier MERLE
Collaborations : Paola CINNELLA (Sorbonne Université, Institut Jean Le Rond d'Alembert), Grégory DERGHAM (Safran Tech)

In the continuity of the work carried out in previous years on the use of mixtures of turbulence models to improve the prediction of RANS calculations, two new approaches have been developed within the framework of the theses of Maximilien de Zordo-Banliat and Soufiane Cherroud.

In the first case, the method of Bayesian mixing of models and scenarios (BMSA) used by Maximilien imposes the weights associated with each model to be constant. This constraint imposes the same ranking on the models everywhere in the flow and limits the precision of the predictions. It is therefore a question of endowing the weightings of the models with a spatial dependence, taking inspiration from the work of Yu et al. on Clustered Bayesian Averaging. Moreover, to allow the generalization of the weights learned on specific geometries, this spatial dependence is imposed on a space of features supposed to represent the characteristics of the flow. The method has been successfully applied, in a turbomachine case, on the NACA65 v103 cascade.

In the second case, and following the work of Schmeltzer et al., it is to symbolically identify a corrective term to the Reynolds tensor. To do this, a corrective term integrity basis was developed based on Pope's decomposition. The coefficients of the decomposition are then sought by the SBL method, which makes it possible to select only the most relevant vectors from the base, while providing the coefficients of the decomposition with probability distributions. By doing so, it becomes possible to propagate these distributions through a RANS computer code, using a polynomial chaos decomposition, to quantify the uncertainties on the prediction. The method has so far been applied to the k-omega SST model on separated flows of the convergent-divergent type, periodic hills and bumps.

Publications et communications :

[1] de Zordo-Banliat, M., Merle, X., Dergham, G., and Cinnella, P., "Estimates of turbulence modeling uncertainties in NACA65 cascade flow predictions by Bayesian Model-Scenario Averaging", Aero2020+1, Poitiers, France, April 12-13-14 2021.

[2] de Zordo-Banliat, M., Dergham, G., Merle, X., and Cinnella, P., "Space-dependent Bayesian model averaging of turbulence models for compressor cascade flows", UNCECOMP 2021, on-line, June 29-29-30 2021.

Quatrième partie

Instabilités, Transition & Contrôle (ITC)

`dNami` : a framework for solving systems of balance laws using explicit numerical schemes on structured meshes'

Nicolas Alferez
Collaboration : Emile Touber (OIST, Japan)

The time evolution of a variety of physical and biological processes may be described by systems of balance laws, which, if given appropriate initial and boundary conditions, dictate the future states of the systems. For instance, systems of balance laws invoking mass, momentum and energy have been incredibly successful at providing meaningful insights to the future states of realistic systems in physics (e.g. fluid dynamics). Yet, experimenting numerically with such systems still requires much implementation time. `dNami` (di :na :mi :) was created so that more research time is spent exploring the dynamical properties of the system of balance laws of interest to the user, and less time is wasted on its numerical implementation across the whole computational spectrum, from the initial small-scale exploratory work on a workstation to the final large-scale computations on national clusters. Thus, `dNami` is a computational framework to study problems of the form :

$$\frac{\partial \mathbf{q}}{\partial t} = f(\mathbf{q}) \; + \; \text{initial/boundary conditions}, \tag{1}$$

in a flexible and efficient manner, where $\mathbf{q} \in \mathbb{R}^n$ is a vector of n real-valued unknowns, t is time, and $f(\mathbf{q})$ is a generic function of $\mathbf{q}$ which may include differential and algebraic operators.

The ability of `dNami` to clearly separate the problem statement from its numerical implementation (often a major time sink in research laboratories) is rooted in the flexibility of the Python language so as to let the user define her/his own system of balance laws in the most natural way (i.e. using a human-readable syntax), which is then interpreted in Fortran to build a computationally-efficient library of (1) which is callable from Python. Users can then easily interact with their own system of balance laws, including at runtime, thereby making it possible to integrate solutions to (1) with other tools and libraries (e.g. optimisation and stability tools) to fully explore the properties of the system, seamlessly from small to large-scale calculations. At the core of `dNami` is the translation of symbolic expressions written in high-level Python language to discretise equations in low-level Fortran language. `dNami` employs explicit schemes to discretise differential operators.

The source-to-source translation is performed by a set of Python functions using regular expressions. The produced discretised version of (1) is then inserted into appropriate do-loops included in Fortran template files by pre-processing techniques. This simple yet effective strategy makes it possible for the HPC-layer to be tailored at the template-file level independently of (1). Finally, the resulting Fortran source code is compiled as a shared library and optimised through the auto-optimisation process of modern Fortran compilers. A Python module is then created with a high-level interface of the shared library functions using F2PY. It is important to stress that researchers can still follow a traditional development workflow, in a pure Fortran environment, either at the shared library level or inside the high-level interface. `dNami` is published as open-source in Zenodo.

Linear and nonlinear optimal growth mechanisms for generating turbulent bands

Jean-Christophe ROBINET, Enza PARENTE (doctorante/Politecnico di Bari)
Collaborations : S. CHERUBINI (Politecnico di Bari)

Recently, many authors have investigated the origin and growth of turbulent bands in shear flows, highlighting the role of streaks and their inflectional instability in the process of band generation and sustainment. Recalling that streaks are created by an optimal transient growth mechanism, and motivated by the observation of a strong increase of the disturbance kinetic energy corresponding to the creation of turbulent bands, we use linear and nonlinear energy optimizations in a tilted domain to unveil the main mechanisms allowing the creation of a turbulent band in a channel flow.

Linear transient growth analysis shows an optimal growth for wavenumbers having an angle $\sim 35^o$, close to the peak values of the premultiplied energy spectra of direct numerical simulations. This linear optimal perturbation generates oblique streaks, which, for a sufficiently large initial energy, induce turbulence in the whole domain, due to the lack of spatial localization. Whereas, spatially-localized perturbations obtained by adding nonlinear effects to the optimization or by artificially confining the linear optimal to a localized region in the transverse direction, are characterized by a large-scale flow and lead to the generation of a localised turbulent band. These results suggest that two main elements are needed for inducing turbulent bands in a tilted domain : i) a linear energy growth mechanism, such as the lift-up, for generating large-amplitude flow structures, which produce inflection points ; ii) spatial localisation, linked to the presence or generation of large-scale vortices. We finally show that these two elements alone are able to generate an isolated turbulent band also in a large, non-tilted domain.

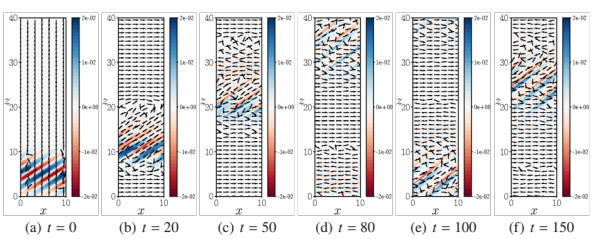

FIGURE 12 – Time evolution of the artificially-localised linear optimal perturbation for $\sigma = 2.5$ and $A = 0.05$ at different times : shaded contours of the wall-normal velocity at $y = 0.25$. For visualization purposes the initial perturbation has been shifted towards $z = 0$.

Publications et communications :

[1] E. Parente, S. Cherubini, J.-C. Robinet, P. de Palma, Linear and nonlinear optimal growth mechanisms for generating turbulent bands, accepted Journal of Fluid Mechanics 2022.

Minimal seeds for turbulent bands in channel flow

Jean-Christophe ROBINET, Enza PARENTE (doctorante/Politecnico di Bari)
Collaborations : S. CHERUBINI (Politecnico di Bari)

In this work, nonlinear variational optimization is used for obtaining minimal seeds for the formation of turbulent bands in channel flow. Using nonlinear optimization together with energy bisection, we have found that the minimal energy threshold for obtaining spatially patterned turbulence scales with $Re^{-8/5}$ for $Re > 1000$.The minimal seed is constituted by a localized spot-like structure accompanied by a low-amplitude largescale quadrupolar structure filling the whole domain. This minimal-energy perturbation of the laminar flow has dominant wavenumbers equal to 0.15 and 4 in the streamwise and spanwise directions, respectively, and is chararacterized by a more marked spatial localization when the Reynolds number increases. At $Re < 1200$, the minimal seed evolves in time creating an isolated oblique band. Whereas, for $Re > 1200$, an almost spanwisesymmetric evolution is observed, giving rise to two distinct bands. A similar evolution is found also at low Re for non-minimal optimal perturbations. This highlights two different mechanisms of formation of turbulent bands in channel flow, depending on the Reynolds number and initial energy of the perturbation. The selection of one of these two mechanisms appears to be affected by the probability of decay of the newly-created stripe, which increases with time, but decreases with the Reynolds number.

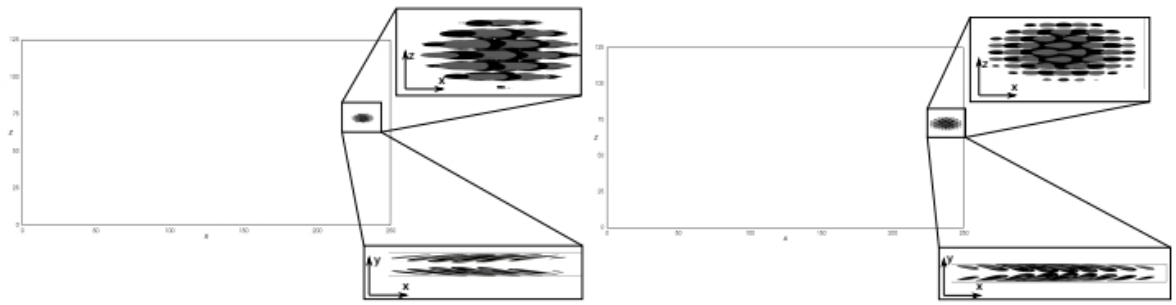

FIGURE 13 – Nonlinear optimal perturbation at time $t = 0$ for different Reynolds numbers with $U_{bulk} = 3/2$ obtained at target time $T = 10$ with the input energy reported in figure 1 by the black dots. Isosurface of the streamwise velocity (light grey for positive and black for negative values, $u' = \pm 0.003$).

Publications et communications :

[1] E.Parente, and J.-Ch. Robinet, P. De Palma and S. Cherubini " Minimal seeds for turbulent bands in channel flow", Journal of Fluid Mechanics, submitted.

Global stability and sensitivity analyses oflow Reynolds number flows around NACA4412 swept wings

J.-C. ROBINET, J.-C. LOISEAU, Gabriele NASTRO (postdoctorant/Univ. d'Orléans)
Collaborations : P.-Y. Passaggia, N. Mazellier (Univ. d'Orléans)

Stability of two- and three-dimensional modes developing on steady spanwise-homogeneous laminar separated flows around periodic NACA 4412 wings for sweep angles between $0° \leq \Lambda \leq 25°$ are numerically investigated using global linear stability theory for different Reynolds numbers and angles of attack. The wake dynamics is attenuated by increasing sweep angles and driven by the two-dimensional von Kármán mode. Its emergence threshold in the $(\alpha - Re)$ plane is computed together with that of the so-called stall mode whose emergence Reynolds number is found to be ~ 1.8 times that of the two-dimensional von Kármán mode. At the critical conditions the Reynolds number, the Strouhal number, the streamwise wavenumber of the von Kármán mode and the spanwise wavenumber of the leading stall mode show a power-law behaviour with respect to the angle of attack. Introducing a sweep angle entails a Doppler effect in the leading modes' dynamics and a shift towards non-zero frequencies of the stall modes which are found to be non-dispersive as opposed to the von Kármán modes. Sensitivity of the leading global modes is investigated in the vicinity of the critical conditions through adjoint-based methods in order to predict regions of the flow which are most sensitive to the application of steady forces. The growth rate sensitivity function displays an extended region on the wing's suction surface close to the leading edge wherein a streamwise oriented force has a net stabilising effect, comparable to the one inside the recirculation bubble. In accordance with the predictions of the sensitivity analysis, a localised spanwise-homogeneous force is found to suppress the Hopf bifurcation and stabilise the entire branch of von Kármán modes.

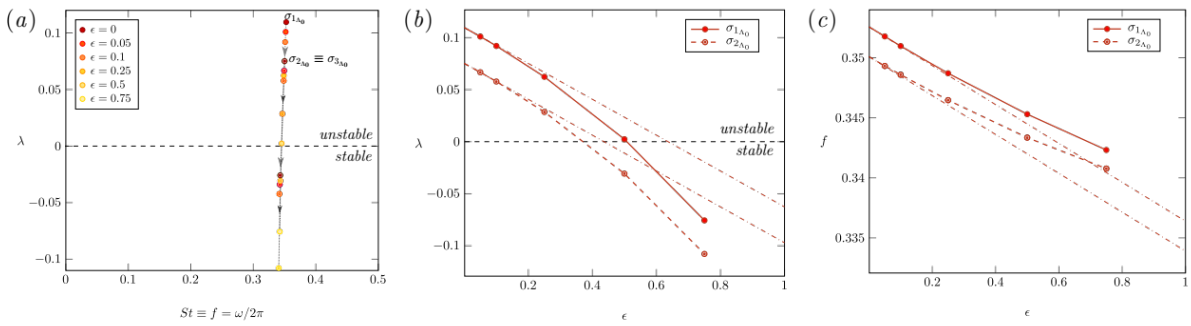

FIGURE 14 – (a) Eigenvalues of the uncontrolled ($\varepsilon = 0$) and controlled flow with a force for increasing ε and located at the station $(x_c{}^\star\,;\, y_c{}^\star)$. The sweep angle is $\Lambda = 0^o$, the angle of attack $\alpha = 20^o$ and the Reynolds number is $Re = 220$; (b) growth rate and (c) frequency as a function of the amplitude ε for the most unstable global modes depicted in (a).

Publications et communications :

[1] G. Nastro, J.-C. Robinet, J.-C. Loiseau, P.-Y. Passaggia, N. Mazellier, "Global stability and sensitivity analyses oflow Reynolds number flows around NACA4412 swept wings", Journal of Fluid Mechanics, submitted.

Transition to turbulence over superhydrophobic surfaces

Jean-Christophe ROBINET, Antoine JOUIN (doctorant/Politecnico di Bari)
Collaborations : S. CHERUBINI (Politecnico di Bari)

Les surfaces superhydrophobes sont des surfaces texturées composées d'une couche de gaz piégée par des rugosités microscopiques réparties au niveau de la paroi. De telles surfaces présentent des propriétés intéressantes telles qu'une réduction de la traînée turbulente ou un retard dans la transition vers la turbulence.

Ce travail se concentre sur ce dernier aspect pour les rugosités de riblet superhydrophobes orientées comme dans Pralits et al. 2017. La surface est modélisée avec un ensemble de conditions aux limites effectives. La technique d'homogénéisation est adaptée de celle pour les surfaces rugueuses décrite dans Zampogna et al. (2019) et Bottaro & Naqvi 2020. Les conditions aux limites effectives donnent un écoulement de base de la forme $\mathbf{U} = [U(y); 0; W]^T$ sur lequel une analyse de stabilité modale et non modale est réalisée. Le théorème de Squire n'est plus valide et une forte asymétrie de la courbe neutre autour de l'axe $\beta = 0$ peut être observée sur la figure 15. La croissance transitoire est également affectée : le gain maximum est obtenu pour un α petit mais non nul et pour $\beta < 0$. Les perturbations initiales optimales sont toujours composées de vortex contrarotatifs, mais les stries dans la composante de vitesse dans le sens du courant sont maintenant obliques. La transition vers la turbulence est étudiée par simulation numérique directe (DNS). La transition pour les deux types de mode à $Re = 5000$ est considérée pour étudier l'influence de l'orientation des riblets dans le délai de transition. Pour les petites longueurs de glissement, les structures cohérentes sont similaires à celles trouvées dans l'écoulement plan de Poiseuille. Les épingles à cheveux présentent une asymétrie et les deux jambes sont étirées dans le sens du courant. Pour des longueurs de glissement plus importantes, le scénario de transition est radicalement différent : les mécanismes modaux produisent des stries (modulations de vitesse alignées dans le sens des courants) près des parois et l'instabilité secondaire de ces stries conduit à la rupture turbulente de l'écoulement.

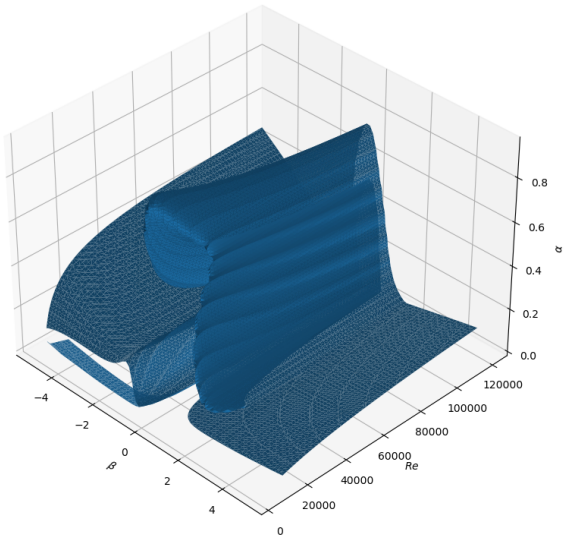

FIGURE 15 – Courbe neutre 3D pour une taille de rugosité $\varepsilon = 0.03$ et une orientation de riblet $\theta = 45^o$.

Application of 3D-Parabolized Stability Equations to Asymmetric Jets

J.-C. ROBINET, Mateus AVANCI (Doctorant)
Collaborations : P. JORDAN (CNRS/Institut Pprime), G. PONT, J. HUBER (Airbus/AO-SAS)

Hydrodynamic instability analysis has been widely used for predictions of the acoustic field of a jet. The geometry of the jet nozzle is an important factor in the development of instabilities and their acoustic radiations. The present work discusses the development of a numerical code for a 3D-LPSE (Linear Parabolized Stability Equations) instability analysis applied to a jet with an asymmetric elliptical shaped nozzle. For the initialization of the method, the spatial stability analysis BiLocal EVP (Eigenvalue Problem) solutions were used in general curvilinear coordinates with the typical spectral method for calculations. The code was implemented and extensively validated focusing on the case in the literature of a jet with an asymmetric flow profile. For the 3D-LPSE stability analysis the validations were focused on a contra-rotating isolated realistic vortex case. The 3D-LPSE solver is then applied to base flows obtained by numerical simulation, representing elliptical jets with various eccentricity values. The results were also compared using the BiLocal EVP analysis for different points in the domain and the results show a good agreement between both methods. The impact of asymmetry on the most unstable jet modes is discussed.

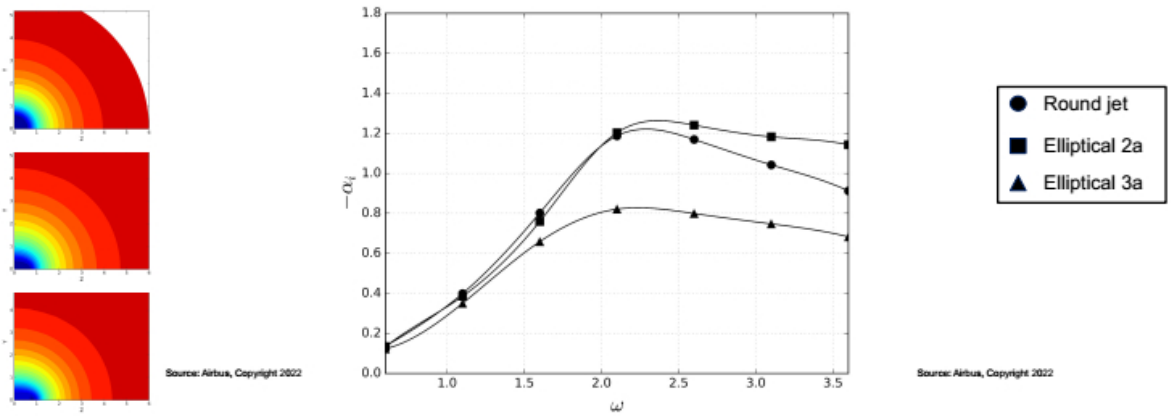

FIGURE 16 – Influence on the linear modal stability of the ellipticity $AR = 1, 2, 3$ (AR : Aspect Ratio) of an adapted subsonic jet. Odd-Even perturbations.

Krylov methods for large-scale dynamical systems : Application in fluid dynamics

J.-C. ROBINET, J.-C. LOISEAU, Ricardo FRANTZ (Doctorant)

In fluid dynamics, the ability to predict and characterize bifurcations from the onset of unsteadiness to the transition to turbulence is of critical importance in both academic and industrial applications. Numerous tools from dynamical system theory can be employed for that purpose, usually resorting to linear stability analyses and ultimately falling in the computation of large-scale eigenvalue problems. In this review, we present a didactically concise theoretical framework focusing on practical aspects of computation and stability analyses of steady and time-periodic solutions with emphasis on very high-dimensional systems such as those resulting from the discrete Navier-Stokes equations. Relying on a matrix-free approach based on Krylov methods, we expand the capabilities and leverage the geometrical flexibility of the open source high performance spectral element-based time stepper Nek5000. The numerical methods discussed are implemented in nekStab, an open source and user-friendly add-on toolbox dedicated to the study of the stability properties of flows in complex three-dimensional geometries. The performance and accuracy of the methods are illustrated and examined on the basis of standard benchmarks from the fluid mechanics literature. Because of its flexibility and domain-agnostic nature, the methodology presented in this work can be applied to develop similar toolboxes for other solvers, most importantly outside the field of fluid dynamics.

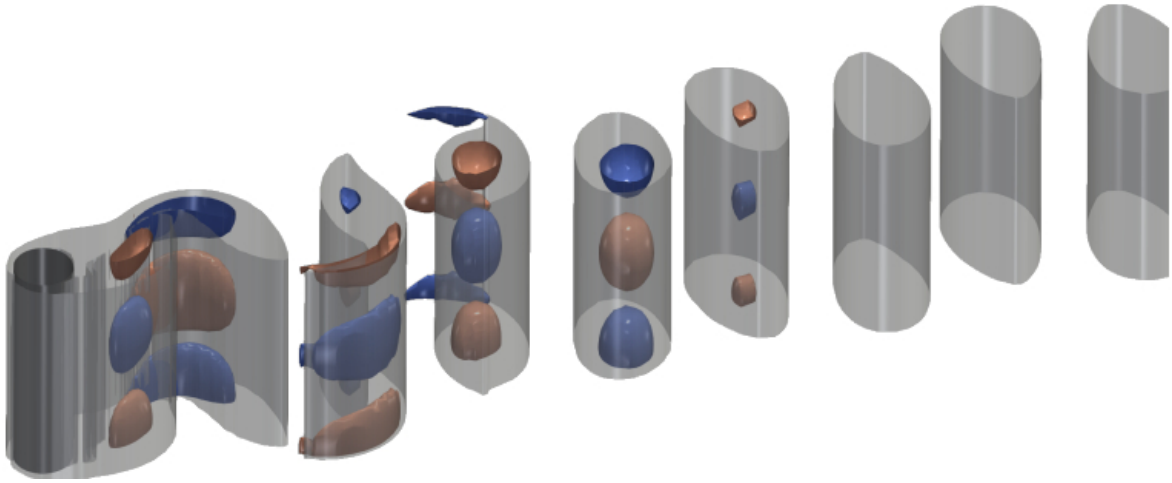

FIGURE 17 – The flow past a circular cylinder : semitransparent vorticity magnitude contours ($\omega = 0.35$) of the limit cycle at supercritical $Re = 190$ superimposed with streamwise vorticity contours ($\omega_x = \pm 0.18$) of the real part of the unstable steady mode.

Publications et communications :

[1] R. Frantz, J.-C. Loiseau, J.-C. Robinet, "Krylov methods for large-scale dynamical systems : Application in fluid dynamics", Applied Mechanical Review, submitted.

Universal sequence of bifurcations on the wake of bluff bodies

J.-Ch. LOISEAU, J.-Ch. ROBINET, R. FRANTZ (Doctorant)
Collaborations : C. Mimeau (M2N/CNAM Paris)

The study of viscous fluids evolving around three-dimensional bluff bodies has attracted much interest in the fluid mechanics literature because of its practical engineering applications. Fundamental studies of the three-dimensional dynamics of canonical bodies such as discs, spheres, and cubes have proved useful in improving the understanding of configurations such as the prototypical Ahmed body or much more complex ones.

Understanding the transition dynamics and instabilities that develop in the flow past bluff bodies is essential. The phenomenon of vortex shedding on three-dimensional bluff bodies, such as a static sphere or cube, has similarities and differences to their two-dimensional counterparts mentioned previously. In the present study, we use the denomination three-dimensional bluff body to refer to a body with finite span and therefore a finite aspect ratio AR, in contrast to two-dimensional geometries such as the circular or square cylinder. As for the circular and square-cylinder cases, the literature on three-dimensional bluff body flows is extensive and includes laboratory, theoretical, and numerical work. The present paper aims at giving some insight into the conjecture of a universal sequence for the first bifurcations experienced by bluff-body flows and to the possible route(s) to chaos. The studies will be performed on two canonical bluff body flows, namely the flow around a static cube and on the flow around a static sphere, using both non-linear analysis and global linear stability with the nekStab open-source toolbox developed for the Nek5000 solver. The flow features and the corresponding physical mechanisms in these flow regimes are explained in more detail.

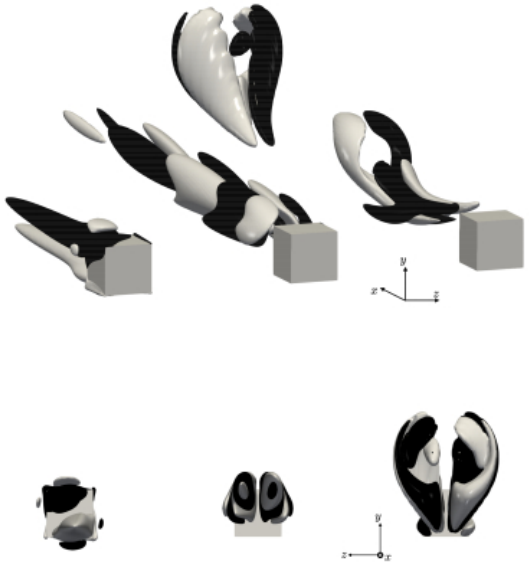

FIGURE 18 – Flow past a cube. 3D and rear back views of isocontours of streamwise vorticity $\omega_x = \pm 0.3$ of the real part of the leading unstable mode at regime II with $Re = 215$ (left), regime III with $Re = 265$ (center), and regime IV with $Re = 282$ (right).

Bifurcation analysis of the jet in cross-flow

J.-Ch. LOISEAU, J.-Ch. ROBINET, R. FRANTZ (doctorant Arts & Métiers)

Cette thématique, en continuité directe avec la précédente, est développée au sein du laboratoire depuis 2018 dans le cadre de la thèse de doctorat de R. Frantz (contrat ministériel) et s'intéresse aux mécanismes d'instabilité et de transition au sein d'écoulements pour lesquels l'état de base présente une dynamique périodique en temps. De tels écoulements peuvent résulter d'une bifurcation primaire (e.g. dynamique de type *oscillateur auto-entrenu*) ou bien d'un forçage extérieur (e.g. *oscillateur forcé harmoniquement*) comme dans le cas des actuateurs à jet pulsé dans des perspectives de contrôle.

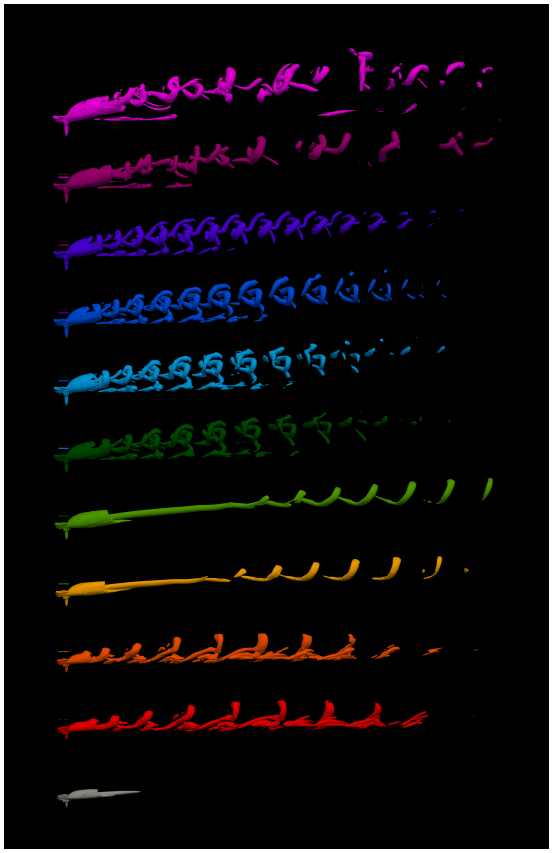

FIGURE 19 – Visualisation λ_2 des tourbillons dans le sillage d'un jet pénétrant une couche limite. Le rapport de vitesse entre le jet et la couche augmente du bas vers le haut.

A titre d'exemple, la figure ci-contre illustre l'évolution des tourbillons se développant dans le sillage d'un jet pénétrant une couche limite pour divers rapports de vitesse. Au fur et à mesure que le rapport de vitesse entre le jet et la couche limite incidente augmente, la typologie et la dynamique des tourbillons dans le sillage évolue, passant d'une absence de tourbillon à faible rapport à un lâcher périodique pour des rapports intermédiaires. Lorsque ce rapport augmente encore, le lâcher perd sa dynamique périodique et l'écoulement transitionne alors vers un comportement chaotique réminiscent de la turbulence. C'est afin de mieux comprendre ce changement de dynamique que l'équipe ITC poursuit les développements algorithmiques initiés dans le précédent axe de recherche afin de les adapter à des états de base périodiques en temps. Elle s'inspire notamment des outils classiquement utilisés en théorie des systèmes dynamiques et les adapte au cas particulier de la dynamique des fluides en les implémentant dans des solveurs Navier-Stokes hautes performances tels que Nek5000.

Tout comme pour la thématique précédente, une attention particulière est portée à l'étude d'écoulements pleinement tri-dimensionels qui, bien que simplifiés, présentent des intérêts applicatifs évidents tels que celui présenté sur la figure ci-contre ou bien celui induit par un jet pulsé, i.e. un type d'actuateur régulièrement utilisé dans des optiques de contrôle et de réduction de la traînée en aérodynamique.

Global Stability Analysis Of Industrial Compressible Fluid Flows

Jean-Christophe ROBINET, Valentin FER (doctorant/ONERA)
Collaborations : C. CONTENT, S. BENEDDINE, D. SIPP (ONERA-Meudon/DAAA)

Les écoulements dans des configurations industrielles sont généralement géométriquement complexes avec des dynamiques très riches. L'émergence de phénomènes instationnaires auto-entretenus est généralement liée à la naissance d'au moins un mode propre instable. La compréhension de l'origine fine de cette dynamique temporellement auto-entretenue, de même que sa modélisation, peuvent ainsi être améliorées par une étude de stabilité linéaire. Les techniques mises en œuvre pour ce type d'analyse consistent en la résolution de systèmes aux valeurs propres doivent alors être étendues à des configurations complexes. Cette résolution peut être réalisée par des méthodes de Krylov avec des transformations spectrales de type shift-and-invert, qui nécessitent des inversions de matrices creuses de très grandes dimensions.

Mais dès lors que l'on considère des cas 3D dépassant les 10^7 degrés de liberté (d.d.l.) comme le compresseur CME2, les techniques d'inversions directes de type LU ou QR deviennent trop coûteuses en mémoire (de l'ordre de $N^2_{d.d.l.}$). Un choix possible est alors de se porter sur des méthodes itératives, et en particulier l'algo. GMRES, du fait de la non symétrie, de la non normalité et de la non diagonale dominance des opérateurs à inverser. Pour bénéficier des travaux récents sur l'inversion efficace de grands systèmes creux en arithmétique réelle, il convient de réécrire le système complexe issu du problème aux valeurs propres en système réel équivalent. L'objectif de ce travail est donc d'étendre à la résolution de problèmes aux valeurs propres les développements récents en vue de mener une analyse de stabilité sur le CME2. La figure 20 présente le gain optimal du resolvent pour un profil supercritique OAT15A dans une configuration de tremblement transsonique sous-critique. L'objectif de ces travaux est de les étendre à des configurations 3-D.

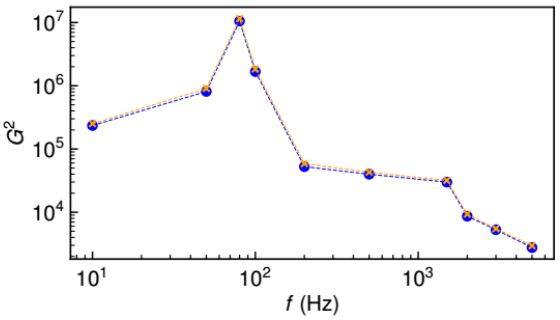

FIGURE 20 – OAT15A profil : optimal gain computed with SLEPc and elsA for subcritical AoA $\alpha = 7^o$. Peaks at $f = 80$ Hz (buffet) and $f = 1500$ Hz (Kelvin-Helmholtz).

Cinquième partie

Publications

Publications - Communications

— ACL

[1] Alferez, Nicolas, Touber, Emile, Winn, Stephen, Ali, Yussuf. (2022). dNami : a framework for solving systems of balance laws using explicit numerical schemes on structured meshes (Version 2). Zenodo. https ://doi.org/10.5281/zenodo.6720593

[2] S. Cherubini, F. Picella, J.-C. Robinet " Variational Nonlinear Optimization in Fluid Dynamics : The Case of a Channel Flow with Superhydrophobic Walls ", Mathematics - 2021 - Vol. 9, 53

[3] R. Ranjan, S. Unnikrishnan, J.-C. Robinet, D. Gaitonde " Global transition dynamics of flow in a lid-driven cubical cavity " Theoretical and Computational Fluid Dynamics - 2021 - Vol. 35 - pp. 397-418

[4] A. Bucci, S. Cherubini, J.-C. Loiseau, J.-C. Robinet " Influence of freestream turbulence on the flow over a wall roughness " Physical Review Fluids - 2021 - Vol. 6, 063903

[5] C. Gouin, C. Junqueira Jr., E. Goncalves, J.-C. Robinet " Numerical investigation of three-dimensional partial cavitation in a Venturi geometry " Physics of Fluids - 2021 - Vol. 33, 063312

[6] E. Parente, M. Farano, J.-Ch. Robinet, P. De Palma and S. Cherubini "Continuing invariant solutions towards the turbulent flow" Phil. Trans. R. Soc. A, 2021

[7] J.-Ch. Loiseau, S. L. Brunton and B. R. Noack."From the POD-Galerkin method to sparse manifold models." Handbook of Model Order Reduction, vol. 3, 2021.

[8] J. L. Callaham, S. L. Brunton and J.-Ch. Loiseau. "On the role of nonlinear correlations in reduced-order modeling." Accepted for publication in Journal of Fluid Mechanics, 2021.

[9] J. L. Callaham, J.-Ch. Loiseau, G. Rigas and S. L. Brunton. "Nonlinear stochastic modelling with Langevin regression.", Proc. R. Soc. A **477** :20210092, 2021.

[10] L. Vienne , S. Marié. "A Lattice Boltzmann study of miscible viscous fingering for binary and ternary mixtures" Physical Review Fluids, 2021, Vol 6(5), 053904

[11] C. Mimeau , S. Marié , I. Mortazavi. "A comparison of semi-Lagrangian Vortex method and Lattice Boltzmann method for incompressible flows" Computers and Fluids, 2021, Vol 224, 104946

[12] L. Charrier, M.Jubera, G. Pont, S. Marié, P. Brenner, F. Grasso. "Simulations of reactive supersonic/subsonic flow interactions for space launcher applications", International Journal of Numerical Methods for Heat Fluid Flow, Vol. 31 No. 11, pp. 3245-3260, 2021.

[13] Ben Hassan Saïdi, I., Schmelzer, M., Cinnella, P., and Grasso, F., "CFD-driven Symbolic Identification of Algebraic Reynolds-Stress Models", Journal of Computational Physics, Volume 457, 15 May 2022, 111037.

[14] V. Daru, C. Weisman, D. Baltean-Carlès H. Bailliet, « Acoustically induced thermal effects on Rayleigh streaming », J. Fluid Mech. vol. 911, A7, 2021.

[15] V. Daru, C. Weisman, D. Baltean-Carlès H. Bailliet, « A numerical study of the coupling between Rayleigh streaming and heat transfer at high acoustic level », J. of Acoustic Society of America 150(6), p. 4501-4510, 2021.

— **C-ACTI**

[1]

— **C-ACTN**

[1]

— **C-COM**

[1] R. Schuh Frantz, J.-Ch. Loiseau and J.-Ch. Robinet. "Floquet analyses of complex 3D flows." APS 74th Annual Meeting of the Division of Fluid Dynamics, Phoenix, USA, Nov. 2021.

[2] J.-Ch. Loiseau, R. Schuh Frantz and J.-Ch. Robinet. "nekStab : open-source toolbox for large-scale stability analysis in Nek5000." APS 74th Annual Meeting of the Division of Fluid Dynamics, Phoenix, USA, Nov. 2021.

[3] J. L. Callaham, S. L. Brunton and J.-Ch. Loiseau. "On the role of nonlinear correlations in reduced-order modelling." APS 74th Annual Meeting of the Division of Fluid Dynamics, Phoenix, USA, Nov. 2021.

[4] Ben Hassan Saïdi, I., Cinnella, P., and Grasso, F., “CFD-driven Sparse Identification of Algebraic”, Aero2020+1, Poitiers, France, April 12-13-14 2021.

[5] Ben Hassan Saïdi, I., Cinnella, P., and Grasso, F., “Turbulence modeling using CFD-driven Symbolic Identification”, Euromech colloquium, Paris, France, June 16-17-18 2021.

— **C-INV**

[1] J.-Ch. Loiseau. "Instability and transition in three-dimensional boundary layers." Journée Fluides et Couches limites à Cergy, Université de Cergy-Pontoise, Juin 2021.